

A 2 High Energy Hadron Reactions, Spin Dependence

A. YOKOSAWA

Argonne National Laboratory

The summary of Session A2, high-energy hadron reactions, spin dependence, consists mainly of the following talks:

Experiments at Argonne ZGS, presented by Y. Watanabe and A. D. Krisch; experiments at very high energies at Fermilab and CERN presented by M. E. Zeller and M. Steur respectively; high p_{\perp} experiment at CERN by K. Kuroda; KN charge-exchange experiment at CERN by A. de Lesquen; and experiments at KEK presented by K. Miyake.

Polarized-Beam and/or Polarized-Target Experiments I

1. Experimental Determination of pp Elastic-Scattering Amplitudes, and Evidence for $A_1(1^{++})$ and $\epsilon(0^{++})$ Exchanges

A. Introduction

An extensive program has been undertaken by Auer *et al.* to determine proton-proton elastic-scattering amplitudes.¹ There are five independent amplitudes to describe proton-proton elastic scattering, *i.e.*, N_0 , N_1 , N_2 , U_0 and U_2 , which have definite quantum numbers exchanged at asymptotic energy.² The subscripts correspond to the total s -channel helicity flip, and $N(U)$ stands for natural (unnatural)-parity exchange. (Note that U_0 corresponds to A_1 exchange and non asymptotic contribution from the pomeron has a factor $-t/s$, *i.e.*, vanishes at $t=0$.³) They are defined in terms of more familiar s -channel helicity amplitudes $\phi_1, \phi_2, \phi_3, \phi_4$, and ϕ_5 . Experimental observables are expressed in bilinear form in terms of these amplitudes.¹ The observables can be written as $(B, T; S, R)$, where B, T, S and R represent the spin direction of the beam, target, scattered and recoil protons respectively. The spin direction N

is defined as the normal to the scattering plane, L along the direction of motion of the proton being considered, and $S=N \times L$. The spin direction of the beam emerged from Argonne's ZGS is in N direction. By using a superconducting solenoid, the spin direction is rotated from the N to the S direction, and by a bending magnet of vertical field, the spin direction can be further precessed to L direction.⁴ There are two types of polarized-target magnets, one providing L and S spin directions, and one with N direction. The spin of recoil protons can be measured in N and S directions.

B. Determination of amplitudes

The determination of amplitudes require at least 9 measurements because each consists of real and imaginary parts and the overall phase remains arbitrary. When the amplitude N_0 is assumed to be dominant and to have only an imaginary part, then the other amplitudes are determined through the interference with N_0 . Table I gives how each amplitude is related to observables under this assumption. At 6 GeV/ c , enough measurements have been

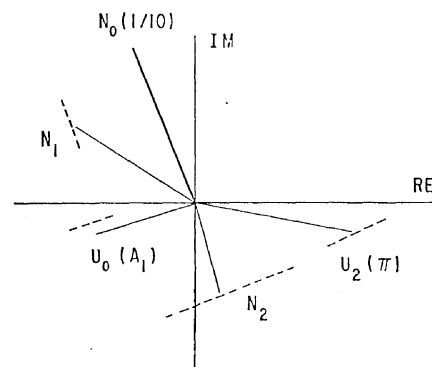


Fig. 1. Preliminary results of amplitude analysis for pp elastic scattering at 6 GeV/ c at $|t| \approx 0.3$ (ref. 1).

Table I. The amplitude and observables

Amplitude	N_0	$\text{Re } N_1$	$\text{Im } N_1$	$\text{Re } N_2$	$\text{Im } N_2$	$\text{Re } U_0$	$\text{Im } U_0$	$\text{Re } U_2$	$\text{Im } N_2$
Observables	$d\sigma/d\Omega$	P	D_{SS}	H_{NSS}	C_{NN}	H_{LSN}	C_{LL}	H_{SNS}	C_{SS}

made to enable full amplitude analysis. Preliminary amplitude analysis has been done and the results are shown in Fig. 1.

C. Evidence for $A_1(I^{++})$ exchange

Berger *et al.*³ made theoretical analysis using experimental data, and concluded the necessity of low-lying trajectories, $A_1(I^{++})$ and $\epsilon(0^{++})$. The evidence for A_1 exchange is primarily indicated from the measurement of $\Delta\sigma_L$, proton-proton total cross-section difference for longitudinal spin states.

$$\Delta\sigma_L = \sigma^{\text{Tot}}(\rightarrow) - \sigma^{\text{Tot}}(\leftarrow) \propto \text{Im } U_0(0).$$

Note that the contribution of the pomeron in the amplitude U_0 vanishes at $t=0$. As shown in Fig. 2, the relatively large values of $\Delta\sigma_L$

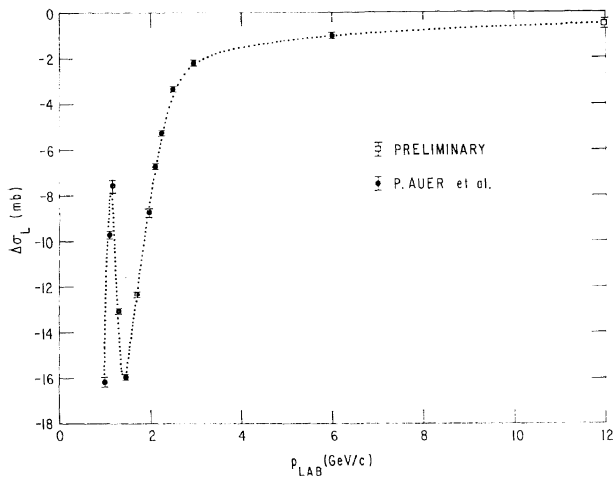


Fig. 2. The values of $\Delta\sigma_L$, proton-proton total cross section difference in the longitudinal spin states as a function of p_{lab} . The dashed line is to guide the eyes.

observed $p_{\text{lab}} \gtrsim 3$ GeV/c is found to be consistent with the one expected from the A_1 trajectory. The remarkable structure at lower energy is discussed in Tsarev's Rapporteur talk and also by A. Yokosawa in Session A5. The need for the A_1 trajectory has been more directly identified through the reaction $\pi^-p \rightarrow \rho^0n$ at 17.2 GeV by CERN-MUNICH collaboration.⁵ Note that in this reaction, the charge is exchanged, and isoscalar trajectories do not contribute. They have investigated this process for sometime, and used a polarized-proton target recently. They saw a fairly big asymmetry even at small t , where π -exchange is known to be dominant. This immediately implies the simultaneous presence of other amplitude with equal naturarity. A part of

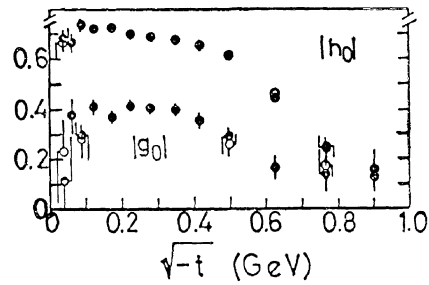


Fig. 3. The results of an amplitude analysis for the reaction $\pi^-p \rightarrow \rho^0n$. The difference between $|g_0|$ and $|h_0|$ implies the existence of A_1 exchange (ref. 5).

their extensive amplitude analysis is shown in Fig. 3, where magnitudes of amplitudes $|h_0|$ and $|g_0|$ are displayed as a function of t . One sees clear difference between $|g_0|$ and $|h_0|$, which contain π and A_1 exchange in opposite sign.

D. pp and pn polarization

The polarizations for pp and pn elastic scattering are expected to show mirror symmetry if $I=1$ trajectory interferes with the pomeron. Up to 12 GeV/c, the pp and pn polarizations are far from mirror symmetry, and to explain the energy dependence, $I=0$ scalar trajectory was necessary.³ The new data from ANNECY-CERN-OXFORD collaboration with polarized proton and deuteron targets at 24 GeV/c are shown in Fig. 4, in which one sees almost mirror symmetry,⁶ indicating that the low-lying trajectory has died away at this energy.

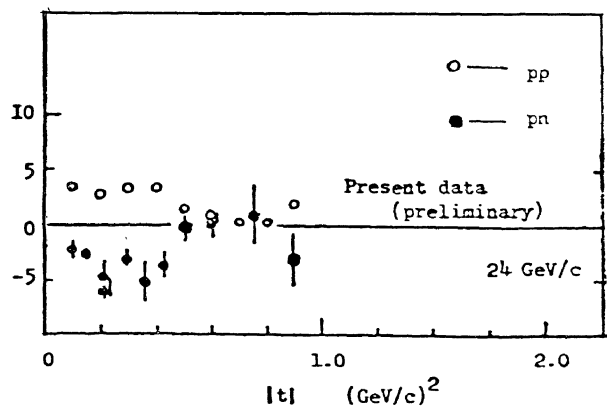


Fig. 4. The pp and pn polarizations at 24 GeV/c (ref. 6).

2. Asymmetry Measurements at High t

The values of C_{NN} parameter in pp elastic scattering has been measured up to 12 GeV/c covering $\theta_{\text{c.m.}} = 90^\circ$ which show unexpectedly

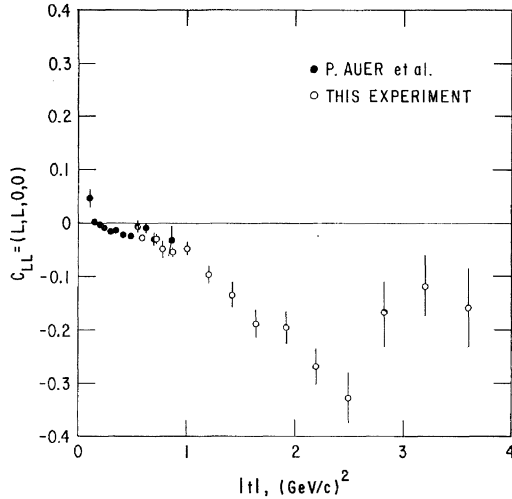


Fig. 5. The correlation parameter C_{LL} vs. t at 6 GeV/c for pp elastic scattering.

large values and interesting structure (see next section, polarized-beams and target experiment II). The measurement of C_{LL} parameter in pp scattering at 6 GeV/c to higher t is shown in Fig. 5.¹ While the values of C_{SL} remains to be small, those of C_{LL} seem to grow with $|t|$ and reach -0.3 and -0.4 . Similarly large effect has been reported by the Minnesota-ANL-Rice collaboration who measured the polarization of pn elastic scattering up to $|t| \approx 8$ (GeV/c)² at 6 GeV/c as shown in Fig. 6.⁷

Finally, the measurement of polarization in pp elastic scattering at 24 GeV/c has been extended up to $|t| = 5$ (GeV/c)² by ANNECY-CERN-OXFORD group.⁶ The results, as shown in Fig. 7 seem to indicate an interesting structure around $|t| = 4$.

M. Sawamoto and S. Wakaizumi have extended the eikonal model to include the spin-

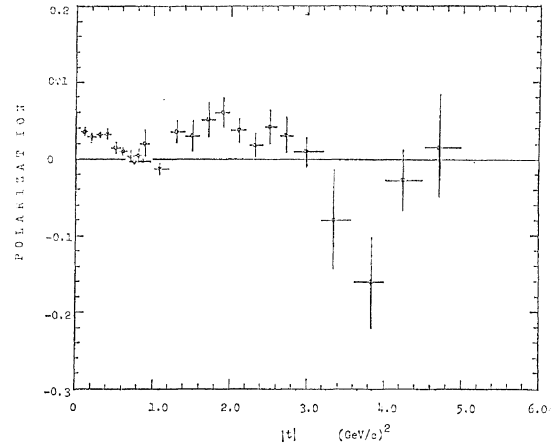


Fig. 7. The polarization of pp elastic scattering at 24 GeV/c for $|t|$ up to 5 (GeV/c)².

orbit (LS) and spin-spin (SS) coupling⁸ and have obtained the relations $C_{SS} = C_{LL}$ and $C_{SL} = 0$, which represent fairly well the data at 6 GeV/c. Fitting the data, they have found that spin-spin force operates deep inside of the proton, which is suggestive of some interesting structure here.

Polarized-Beam and Polarized-Target Experiment II

In this section measurements of C_{NN} (or $A_{NN}) = (N, N; 0, 0)$ at high p_{\perp} are exclusively covered. Last fall O'Fallen *et al.*⁹ measured proton-proton elastic-scattering cross sections at 11.75 GeV/c in pure initial spin states out to $p_{\perp}^2 = 4.2$ (GeV/c)². They found that the spin-spin correlation parameter C_{NN} had a very dramatic rise starting at $p_{\perp}^2 = 3.6$ (GeV/c)² just at the start of the large p_{\perp}^2 hard scattering component of p-p elastic scattering, which is

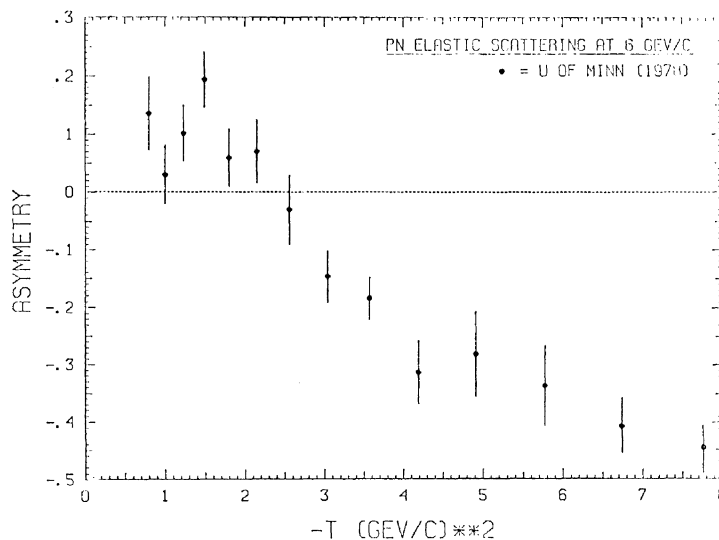


Fig. 6. The polarization of pn elastic scattering up to $|t| = 8$ (GeV/c)² at 6 GeV/c.

seen very clearly at ISR energies.¹⁰ By $P_{\perp}^2 = 4.2$ $(\text{GeV}/c)^2$ the ratio $(d\sigma/dt)_{\uparrow\uparrow}/(d\sigma/dt)_{\uparrow\downarrow}$ had reached a value of almost 2. While it appeared most likely that this large spin-spin force was associated directly with the large- $P_{\perp}^2 e^{-1.6P_{\perp}^2}$ hard-scattering component, it was also possible that it was associated with the interference between the hard-scattering component and the medium- $P_{\perp}^2 e^{-3P_{\perp}^2}$ component.

It now appears much more likely that the large spin-spin interaction is indeed associated with the $\exp(-1.6P_{\perp}^2)$ region itself. This can be seen quite clearly from our very new data, where we extended the measurements of p-p elastic spin effects out to $P_{\perp}^2 = 5.09$ $(\text{GeV}/c)^2$ which is 90°_{cm} at 11.75 GeV/c.¹¹ The ratio $(d\sigma/dt)_{\uparrow\uparrow}/(d\sigma/dt)_{\uparrow\downarrow}$ is plotted against P_{\perp}^2 in Fig. 8. This ratio reaches at least a

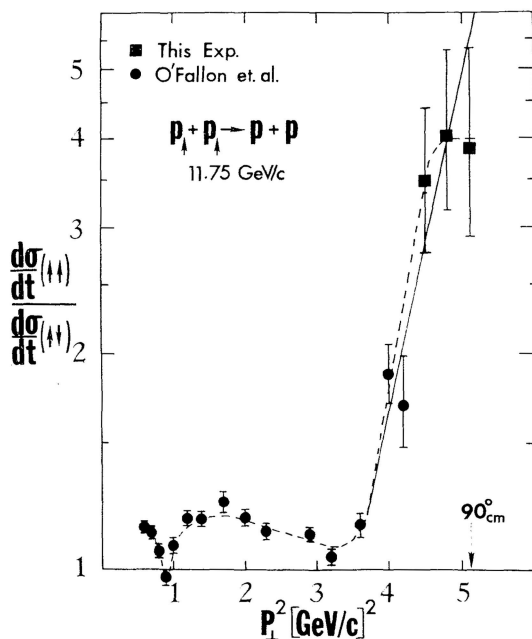


Fig. 8. Plot of the ratio of the differential elastic cross-sections in pure initial-spin states for $p+p \rightarrow p+p$ at $p_{\text{lab}} = 11.75$ GeV/c. The curves are only to guide the eye.

factor of 4 at the maximum P_{\perp}^2 presently available at the ZGS. As can be seen from the dashed and solid lines our present errors are too large to determine if the ratio has reached an asymptotic value of exactly 4 or is still growing. In any case it seems both remarkable and ironic that the largest spin effect ever observed in elastic scattering occurs at the maximum energy and P_{\perp}^2 presently available in the world.

This large spin-spin force in high- P_{\perp}^2 elastic

p-p scattering may be due to the spin dependence of the direct scattering of the constituents of the proton. We do not know the exact nature of these constituents but the slope of 1.6 $(\text{GeV}/c)^{-2}$ corresponds to a size of about $1/3$ Fermi, which may be a measure of the size of the constituents. The large spin-spin force would then indicate that these constituents rarely scatter unless their spins are aligned.

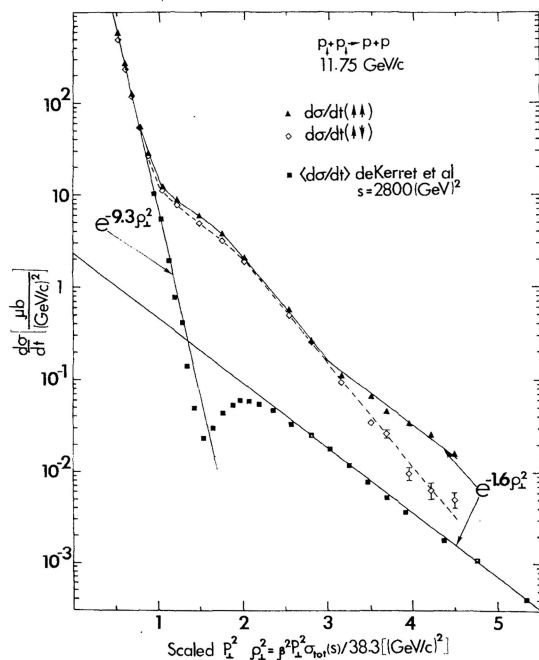


Fig. 9. The 11.75 GeV/c spin dependent proton-proton elastic cross-sections are plotted against ρ_{\perp}^2 .

In Fig. 9 the spin parallel ($\uparrow\uparrow$) and spin antiparallel ($\uparrow\downarrow$) cross sections are plotted against the scaled P_{\perp}^2 variable, ρ_{\perp}^2 , giving an overall picture of spin-spin effects in p-p elastic scattering. From $\rho_{\perp}^2 = 0 \rightarrow 3$ $(\text{GeV}/c)^2$ the two cross sections are quite equal except for a small spreading just near the break at the end of the diffraction peak. The familiar $e^{-1.6\rho_{\perp}^2}$ hard-scattering component, seen in the ISR data,¹⁰ then suddenly appears at $\rho_{\perp}^2 \sim 3$ $(\text{GeV}/c)^2$, but apparently *only* in the spin-parallel cross-section $d\sigma/dt$ ($\uparrow\uparrow$). Our data are consistent with their being *no* hard-scattering break at all when the protons' spins are antiparallel.

This new fact may help us to understand the nature of the proton's constituents. More generally large- P_{\perp}^2 spin effects may give strong constraints on any theory that associates large- P_{\perp}^2 scattering experiments with the fundamental constituents of the proton. The large-

P_{\perp}^2 spin dependence may even suggest which of these theories is useful and which should be abandoned.

Polarization at Very High Energies I

This review is of two high energy experiments recently completed at Fermilab involving recoil-proton polarization measurements in inclusive processes from protons on carbon and protons on hydrogen,¹² and πp and pp elastic-scattering polarization measurements.¹³ We also discuss a paper which describes an impact-parameter model to predict polarization distributions for pp elastic scattering.¹⁴

G. Baranko *et al.* measured proton polarizations for inclusive processes in the internal target area at Fermilab at incident beam energies from 100 to 400 GeV.¹² The reactions studied were $pp \rightarrow p^{\uparrow}X$ and $pC \rightarrow p^{\uparrow}X$, where the final state proton's polarization was measured with a carbon polarimeter. One reason for studying these reactions was to obtain a comparison with the polarization observed in inclusive A production at similar kinematic conditions.¹⁵ We recall that $p_A = -0.28 \pm 0.08$ at P_{\perp} of 1.5 GeV in the region $0.3 < X_F < 0.7$.¹⁶

The apparatus, described in a previous publication,¹⁷ utilized either the hydrogen gas

jet or the rotating carbon target at Fermilab's internal target area. The spectrometer was set so that P_{\perp} values between 0.6 and 1.5 GeV/c were studied at $0.7 < |X_F| < 0.9$.

Figure 10 shows the polarization results from hydrogen and carbon. At this value of P_{\perp} the corresponding A polarization is about -10% , and the small value of polarization from hydrogen indicates that the mechanism which produces polarization of A 's is not effective for the proton. The data are thus inconsistent with prediction of $P_p \simeq -5\%$ from gluon bremsstrahlung models used to explain the A polarization.¹⁸

The absence of polarization in the hydrogen reaction has caused the authors to investigate secondary processes being responsible for polarization effects from carbon. Their tentative explanation is that there is a preferential acceptance of protons which rescatter within the primary carbon target to the left over those to the right. This occurs since the inclusive cross section for fixed momentum favors small angles. A model based on this hypothesis predicts that these rescattered protons could be polarized to the observed level.

The experimental apparatus for the elastic scattering experiment,¹³ a two-arm spectrometer system,¹⁹ was designed for high incident beam

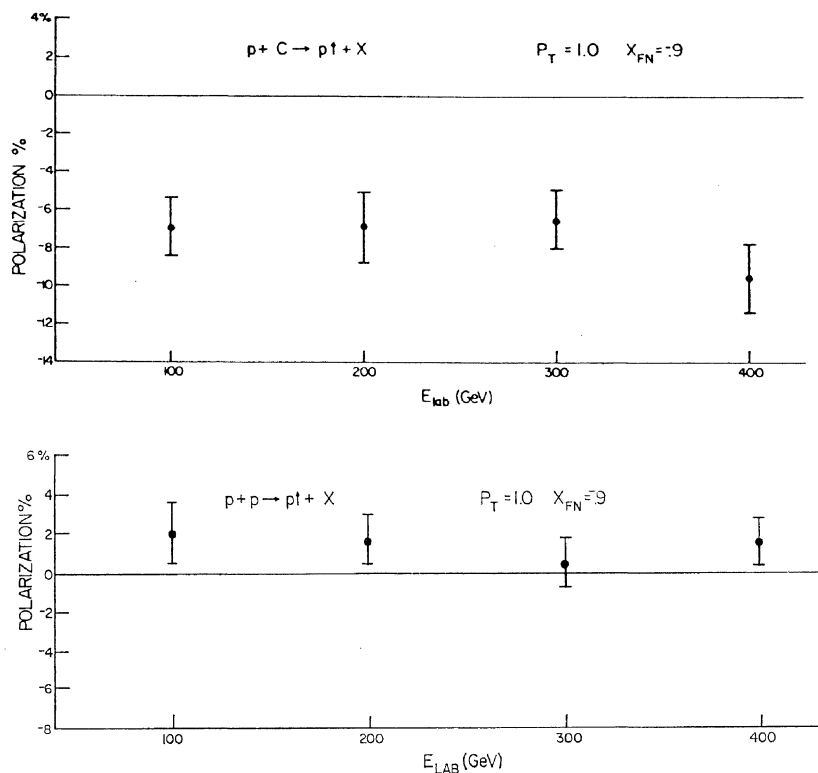


Fig. 10. Recoil proton polarizations from carbon and hydrogen as a function of beam energy.

fluxes and thus had no detectors directly in the beam line. The incident beams were 100 GeV π^\pm mesons and protons, and 300 GeV protons. Cerenkov counters on the forward arm determined the species of the scattered, and thus the incident particles. Determination of the scattered- and recoil-particle trajectories was made with proportional wire chambers placed on either side of superconducting spectrometer magnets on each arm of the apparatus. The signal to background ratios for observation of elastically scattered events ranged from 15:1 at low momentum-transfer values to 1:1 at high.

The authors have compared all of their data to a Reggeized strong absorption model,²⁰ the predictions of which appear as the smooth curves in the following figures. The model has no helicity flip component to the diffractive (pomeron) part of the amplitude.

All angular distributions have been normalized to previously published data around $-t = 0.6$ (GeV/c)² to yield differential cross sections.²¹ The π^+p data agree fairly well with their previously published counterparts, but the π^-p results seem to be too low in the $0.85 < -t < 1.2$ (GeV/c)² region. The shape of polarization distributions is as expected: mirror symmetry between π^+p and π^-p polarizations, and a magnitude that drops approximately as $s^{-1/2}$. The model prediction is consistent with these results.

Angular distributions for pp elastic scattering, compared to published data,²¹ are shown in Fig. 11. There is good agreement between these data, previous results, and the model fits.

Polarization results are displayed in Fig. 12 along with results of the Fermilab internal-target group at 100 GeV. Again, the model gives a good representation of the data. We note, however, the limited statistical accuracy of the 100 GeV results.

We can compare these angular distributions of polarization with recently published results²² from CERN at 150 GeV as shown in Fig. 13. These polarizations, discussed in detail elsewhere in these proceedings, are larger than those of Fermilab. The model prediction, being rather poor at 150 GeV, does seem reasonable at 300 GeV/c. Models employing helicity-flip components to the diffractive am-

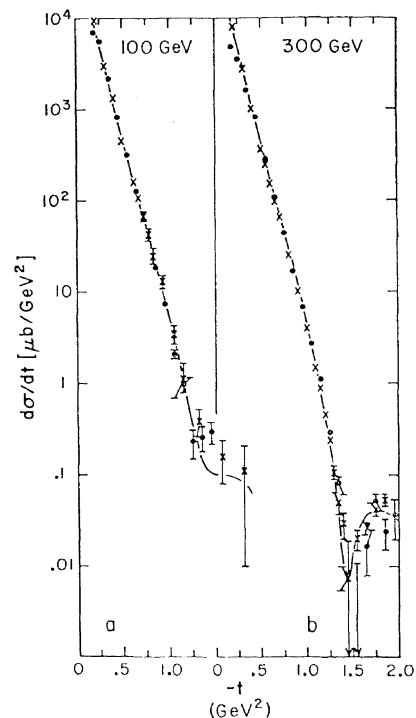


Fig. 11. pp differential cross section. Solid dots are results of this experiment, \times 's are data of ref. 21, smooth curve is discussed in the text.

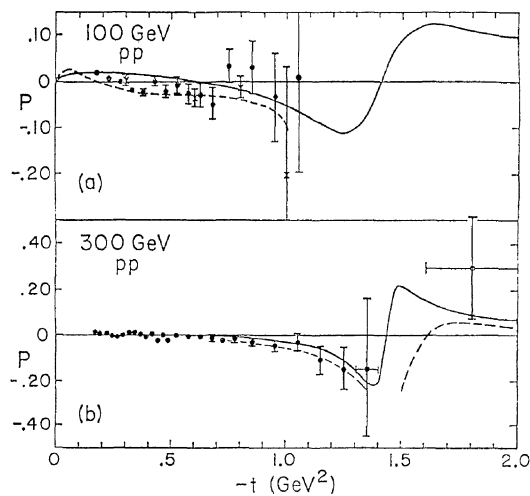


Fig. 12. Polarization data. (a) 100 GeV/c data (dots) plotted with data from ref. 17 (crosses). Dashed curve is a prediction by A.C. Irving (Nucl. Phys. **B101**, (1975) 263), and solid curve is a prediction from ref. 20. (b) 300 GeV/c data. Dashed and solid curves are predictions from refs. 14 and 20 respectively.

plitude^{23,24} fit the CERN data but give poor representations of the Fermilab results, most notably at 300 GeV.

Finally the model which assumes an impact picture¹⁴ using rotation of hadronic matter to give rise to the spin structure of the diffractive amplitudes, is compared with the high energy data in Figs. 12 and 13. These predictions

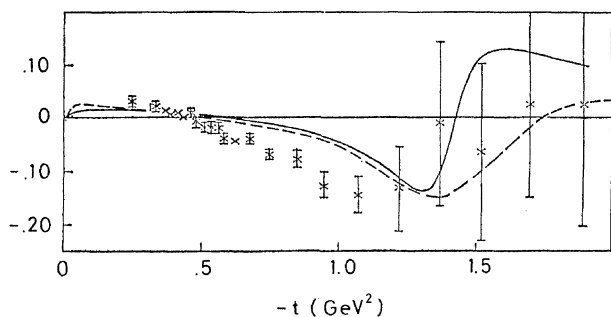


Fig. 13. Polarization data at 150 GeV/c from ref. 22. Dashed and solid are explained in Fig. 12b.

are for the “soft rotation” picture where the velocity of hadronic matter becomes zero as the impact parameter goes to infinity. Further tests of the model can be made by the measurement of the R -parameter distributions which are predicted to be quite structured at high energies.

Polarization at Very High Energies II

In this section, pp polarization measurement at 150 GeV/c by CERN–Padova–Trieste–Vienna collaboration is discussed.²² Two million minimum triggers were collected in the t -range $.2 \leq |t| \leq .3$ (GeV/c)², out of which 420 k survived as pure elastic events. The polarization shows a sizeable negative trend around $|t| \simeq 1$ (GeV/c)², a shape which is apparent in data at 45 GeV/c²⁵ and 300 GeV/c.¹³ The 100 GeV/c data of the latter paper do not, however, provide enough statistical accuracy to draw a clean-cut conclusion on the existence of a polarization. More statistics have been collected at 150 GeV/c which should allow to solve the open question of a second zero-crossing between 1 to 2 (GeV/c)², whereas the first zero crossing around $|t| \simeq .475$ (GeV/c)² is already established. The region for $|t| \geq 1.5$ (GeV/c)² should permit a decision between the eikonal model of Gerhold and Majerotte²⁴ and the impact parametrization of Bourrely, Soffer and Wu.¹⁴

The experiment was performed in the H3-beam of the CERN–SPS, set at 151.6 GeV/c $\pm 1.5\%$ and horizontal and vertical divergences of approximately 0.2 mrad. The beam spot was with FWHM of 6×2.5 mm² well within the polarized target of 22 mm ϕ . Two threshold Cerenkov counters, set on pions, monitored the incident beam of $\simeq 2.5 \times$

10^7 protons per 1.0 sec effective spill time. At a second stage the intensity was increased to around 5.0×10^7 ppp. The target consisted of a 14-cm long propanediol target, polarized to above 90% and a polyethylene (CH₂) disc of 10-mm length \times 22 mm, located 4 cm downstream of the polarized target. This dummy target was essential for the normalization of the spin-up and spin-down runs. A second method used the fact that the average polarization in the region $.4 < |t| < .6$ (GeV/c)² is zero as our data clearly show the zero-crossing.

The experimental set-up consists of two spectrometers, one each for forward and backward particle. The momentum analysis for the forward one is performed by 6.8 T-m where two sets of 4 planes MWPC before and after the magnet fix the directions. The horizontal co-ordinates behind the magnet serve to fix momentum and particle origin within the target by making use of a MWPC-decision logic incorporated in the trigger. Together with a similar logic on the backward arm, this time set on positive particles to suppress negative-particle background we obtain a trigger-reduction of ~ 8 times the scintillator-hodoscope trigger. The polarized-target magnet serves with a 0.95 T-m field from the center onwards to momentum analyze the backward particles with the help of two set of chambers within the magnetic field, one only at 5 cm from the target. Outside the magnet the backward-particle direction is determined by four 100×100 cm² MWPCs. The forward- and backward-arm scintillator hodoscopes behind the last chambers perform the first stage of the trigger.

The data analysis of events was done in three steps: (1) a pattern recognition program requiring at least one track forward and backward arm and checking for consistency with the trigger system. (2) a geometrical fit program requiring to originate backward and forward tracks from a vertex with 1-mm resolution. (3) a kinematical 4c-fit testing the hypothesis of elastic pp scattering by taking account of the incident-beam data. Selecting events with $r < 10$ mm from the polarized-target center and applying a cut of 6% in the χ^2 probability to suppress background leads to the results presented in Figs. 14 and 15.

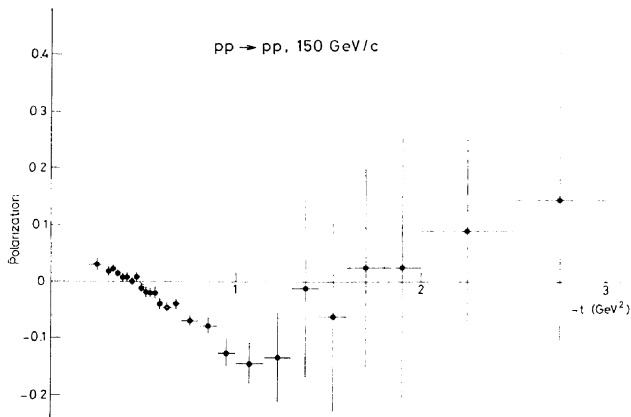


Fig. 14. pp polarization at 150 GeV/c.

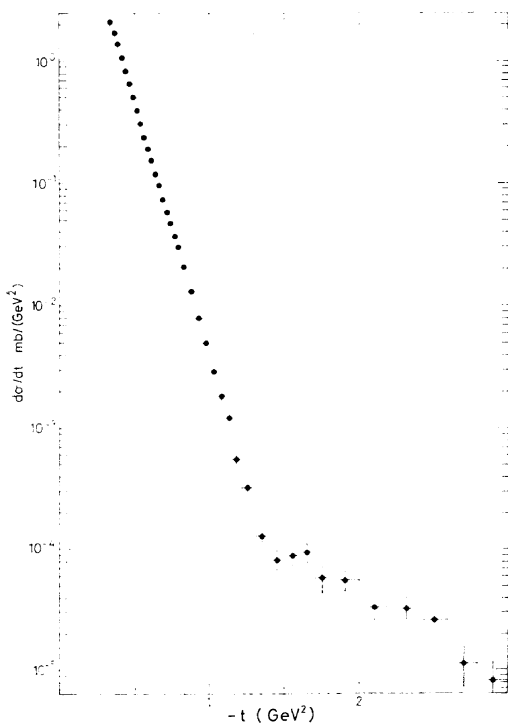


Fig. 15. pp differential cross section at 150 GeV/c.

High P_{\perp} Experiment at CERN

Preliminary results of asymmetry measurements in the inclusive π^0 production at high P_{\perp} were presented.²⁶ This measurement is a part of a series of polarization experiments;

- 1) Polarization parameter in pp elastic scattering,
- 2) Asymmetry in $pp(\uparrow) \rightarrow \pi^0 + \text{anything}$,
- 3) Polarization parameter in pn elastic scattering, which have been performed using a high intensity beam ($10^8 \sim 10^9$ ppp) of 24 GeV/c.

The set-up essentially consists of two lead-glass counters placed at ~ 3 m downstream of a polarized proton target with a production

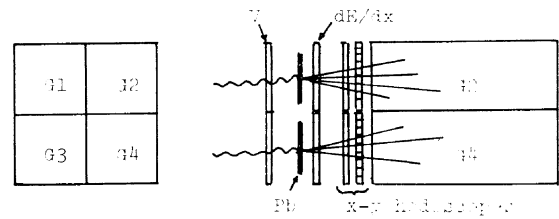


Fig. 16. Experimental setup.

angle of 16° in the lab system corresponding to the central region ($x \sim 0$). As you see here (Fig. 16) each counter consists of 4 blocks of lead-glass in front of which are successively placed a veto counter for charged particles, a Pb converter, a dE/dx -counter and X - Y scintillation hodoscopes. The trigger was defined by a majority coincidence between 2 of 4 $\{\bar{V}_i(dE/dx)_i G_i\}$ with, at least, twice the minimum ionization in the dE/dx counter.

A detailed analysis of data is still in progress, so I present today only very preliminary results without precise estimates of the background. The data used here comes from a pair of blocks only placed on the left-hand side of the beam. We also adopted a simplified analysis ignoring information from the hodoscopes. The momentum of π^0 was, therefore, roughly estimated by means of two small Pb converters specially placed in front of the lead-glass counters.

Essential point of this type of asymmetry measurements, especially at high P_{\perp} region is, of course, the gain stability of lead-glass counters. We therefore carefully checked the difference of gain between "UP" and "DOWN" measurements, and confirmed that it never exceeded 0.15% corresponding to a false asymmetry of $\sim 0.5\%$.

The total asymmetry, without correction for the effective target polarization is plotted in Fig. 17 vs. the transverse momentum of π^0 . Open circles present the results obtained with an inversed magnetic field of the PPT to see the effect of background from charged particles.

Looking at the region inside the geometric acceptance of the counter ($P_{\perp} > 0.9$ GeV/c), the asymmetry decreases rapidly from 0 to $\sim -5\%$ as P_{\perp} increases from ~ 1 to ~ 2 GeV/c. Taking into account the effective polarization of propanediol target the asymmetry for hydrogen events would be about -50% at $P_{\perp} \simeq 1.8$, for example, which seems very

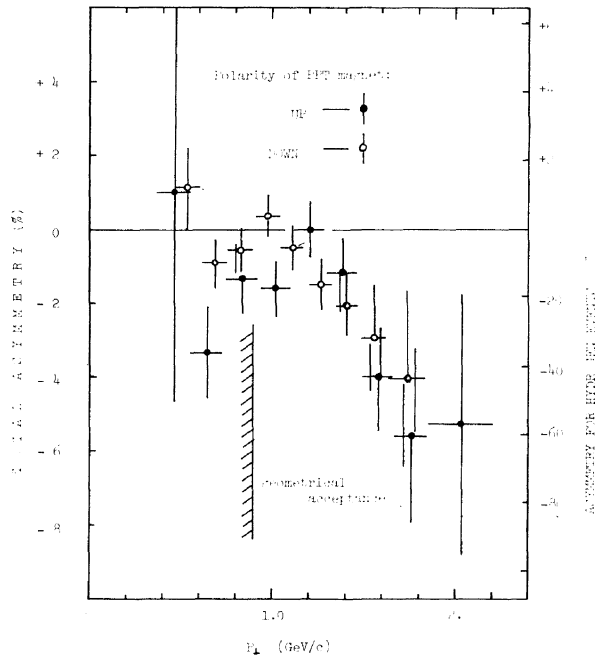


Fig. 17. Asymmetry in inclusive reaction $p+p(\uparrow) \rightarrow \pi^0 + \text{anything}$ in the central region at 24 GeV/c (preliminary results).

important as spin effect at the present incident momentum. This is an important effect and if it is confirmed at higher energies, it should be confronted with test of parton model which only allows small asymmetry at large P_{\perp} .^{27,28}

KN Charge-Exchange Experiment at CERN

Measurements of spin dependent observables are necessary for the experimental determination of two-body hadronic scattering amplitudes and for the understanding of strong interactions. Comparison of the line reversed reactions $K^-p \rightarrow K^0n$ and $K^+n \rightarrow K^0p$ is essential for studying exchange components in Kaon-Nucleon charge exchange. Measurement of the differential cross sections exist for both reactions, but the polarization parameter is only known for $K^-p \rightarrow K^0n$ at 8 GeV/c.²⁹

The recent development of polarized deuteron targets by the CERN polarized-target group made possible the measurements of polarization in $K^+n \rightarrow K^0p$. The target used is 18 g of 92% deuterated propanediol in a cylindrical volume of 120 mm \times 17 mm and placed in a ^3He - ^4He dilution refrigerator. The polarization of deuteron is close to 40% (corresponding to about 37% for the polarization of neutrons).

The K_s^0 emitted forward decay into $(\pi^+\pi^-)$ after a veto counter, and the two pions are

analyzed in a spectrometer of a magnet and 4 wire proportional chambers. The K^0 mass is reconstructed with an error of ± 9 MeV.

The momentum of the recoil proton is measured using the field of the target magnet. The track position is recorded by a hodoscope close to the target, and by two MWPC's. The momentum resolution is $\Delta p/p = 3-4\%$. Two recoil arms are used, left and right, to increase statistics and to minimize the sensitivity to normalization errors.

The events are reconstructed off-line by a CDC 7600 program. From momenta of the incident and the two outgoing particles the Fermi momentum of the target neutron $p_f = p_{inc} - p_p - p_{K^0}$ is calculated with a most probable error of 30 MeV/c. Figure 18 shows the distributions of the reconstructed target momentum for polarized propanediol and carbon targets.

After kinematic cuts ($p_f < 0.25$ GeV/c, $\Delta\theta < 12^\circ$, $\Delta\phi < 12^\circ$) we obtain 13000 events which contain $\simeq 2\%$ of inelastic events on deuterons and about 60% of events on nuclei (carbon and oxygen).

In our result for the polarization in K^+p elastic scattering³⁰ we don't see any structure

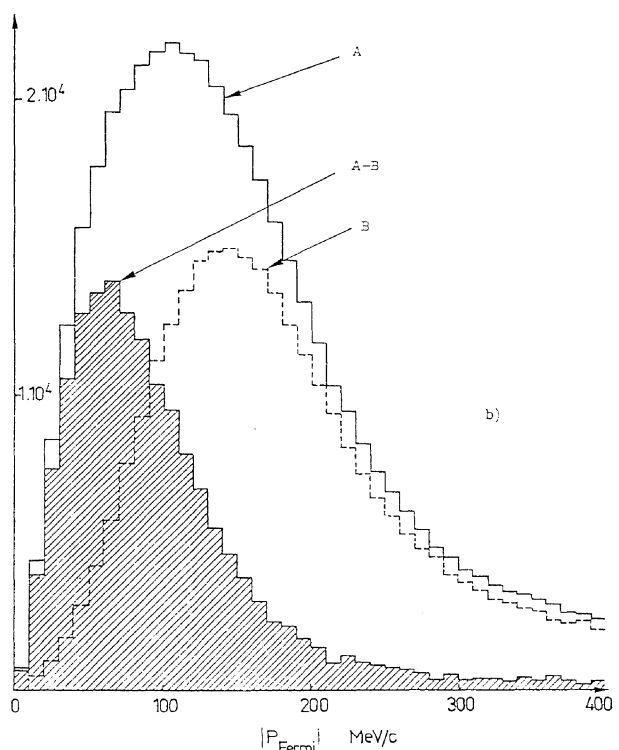


Fig. 18. Distributions of the reconstructed momentum of the target nucleon; events on the polarized target (A) by solid histogram, events on the carbon target (B) by dashed histogram.

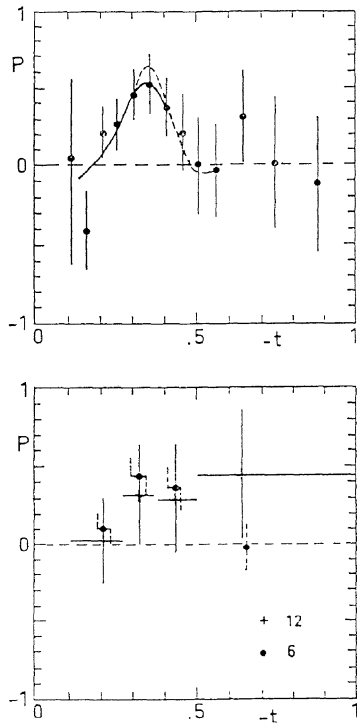


Fig. 19. Results for $P(K^+n \rightarrow K^0p)$ at 6 and 12 GeV/c.

nor any systematic discrepancy with previous data of Borghini *et al.*³¹

In Fig. 19 we show the polarization in $K^+n \rightarrow K^0p$.³⁰ At 6 GeV/c we have analyzed the data in more detail to extract the information on $P(t)$. We have searched for a function $P(t)$ most likely to be represented by all of the events. This method gives a sharp peak of $P \simeq 0.5$ for $|t| \simeq 0.35$ (GeV/c)² and cannot exclude the possibility for negative values for P at $|t| < 0.2$.

This result closes a particular set of observables measured in $K^\pm N$ CEX which allows to solve for the tensor (A_2) exchange components of the s -channel helicity amplitudes in terms of vector (ρ) exchange amplitudes with coefficients now known from data. The A_2 exchange amplitudes can thus be constructed from data with a minimal possible additional assumption that the ρ -exchange amplitudes in K^+N CEX are related to the ρ -exchange amplitudes in πN CEX by SU(3) amplitudes which are well known around 6 GeV/c. $\text{Re } T_0$ and $\text{Re } T_1$ have simple zero at $t = -0.45$ and $t = -0.70$ respectively. $\text{Re } T_0$ has a dip at $t \simeq 0.2$. $\text{Im } T_0$ has a dip of a double zero at $t \simeq -0.2$, and a double zero structure at $t \simeq -0.45$. Violations of weak EXD in both amplitudes correspond to a lower A_2 trajectory

by approximately $\Delta\alpha \simeq 0.1$.

Experiments at KEK

Counter experiments performed at KEK as the first series of experiments were reported. The differential cross sections (DCS) for the π^-p elastic scattering have been measured by Nagoya-Hiroshima-Osaka-Kyoto-KEK collaboration, at eight momenta between 2.1 and 3.5 GeV/c with a step of 0.2 GeV/c and in an angular range of $-0.85 < \cos \theta_{c.m.} < 0.95$.³² The measurements have been made by detecting both pions and protons in coincidence with a large-aperture magnetic spectrometer placed at the forward direction and a WSC system at the other side of the beam. The statistical errors of the present data are less than 10% even at the DCS minimum. In addition to the well-known first dip at $|t| = 0.8$ (GeV/c)² and the secondary peak, two pronounced dips are seen in the large $|t|$ region. These dips have some resemblance to those observed at 3.5 GeV/c.^{33,34}

Polarization parameter, P , in the backward region for the π^-p elastic scattering has been measured by the same collaboration at 2.25, 2.50, 2.75 and 3.50 GeV/c, in a range of momentum transfer $-1.0 \leq u \leq +0.1$ (GeV/c)² with a propanediol polarized target.³⁵ The preliminary results are plotted in Fig. 20 and

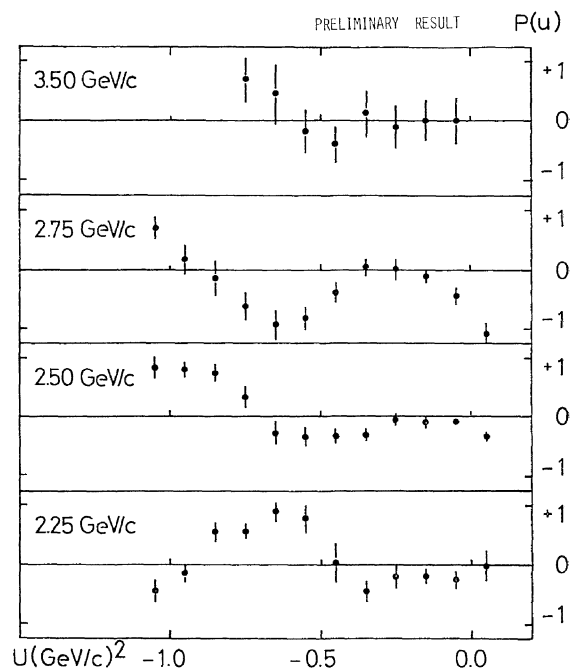


Fig. 20. Preliminary results on the POL for $\pi^-p \rightarrow \pi^-p$ at 2.25, 2.50, 2.75 and 3.50 GeV/c. (Nagoya-Hiroshima-Osaka-Kyoto-KEK.)

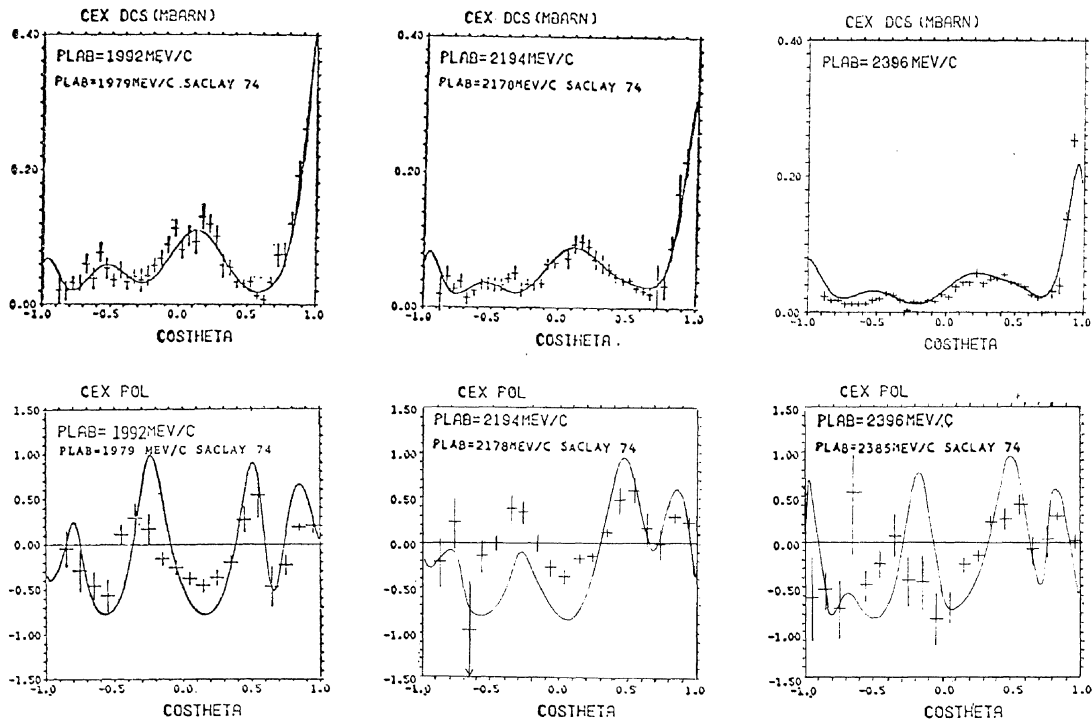


Fig. 21. Preliminary results on the DCS and POL for $\pi^- p \rightarrow \pi^0 n$ at 1.992, 2.194 and 2.396 GeV/c. (Kyoto-Tsukuba-KEK.)

exhibit a profound dip (negative) for 2.25 GeV/c at $u = -0.3$ (GeV/c)², whereas the ANL results at 2.28 GeV/c give positive values.³⁶ This dip has a momentum dependence below 3 GeV/c and disappears at 3.5 GeV/c.

The DCS for the $\pi^- p$ charge-exchange scattering has been measured by Kyoto-Tsukuba-KEK collaboration, at six momenta, 1.992, 2.194, 2.396, 2.596, 2.797 and 2.995 GeV/c and in the angular range of $-0.95 < \cos \theta_{c.m.} < 0.95$.³⁷ The polarization parameter has been measured with an ethylene glycol polarized target at the same momenta except 2.797 GeV/c. Five arrays of lead glass (SF-6) Cerenkov counters of total absorption type combined with lead converters and WSC were placed one side of the beam covering angles of 4° – 130° to measure both the angles and energies of two γ -rays from π^0 mesons. Five arrays of neutron counters were also placed other side of the beam to confirm two-body kinematics of charge-exchange scattering. The part of preliminary results on the DCS and P measurements available at the present are shown in Fig. 21. The present results on the DCS seem to agree with the predictions by Saclay analysis³⁸ and also agree with the LBL data at 1.990 and 2.390 GeV/c. However, there are some differences between the present

results and the Rutherford data³⁹ at 2.267 and 2.724 GeV/c around $\cos \theta_{c.m.} = 0.4$. The polarization results seem to oscillate rapidly as was seen on the LBL and Rutherford data and as indicated by the predictions of Saclay or new Karlsruhe-Helsinki analyses,⁴⁰ and show rather poor quantitative agreements. The present results are expected to give a strong constraint for further phase-shift analyses.

In the polarization measurement of the $\bar{p}p$ scattering at 0.7 GeV/c performed by Tokyo M.U.-Tokyo U.A.T.-Chuo U. collaboration,⁴¹ 3,416 events of $\bar{p}p$ double elastic scattering

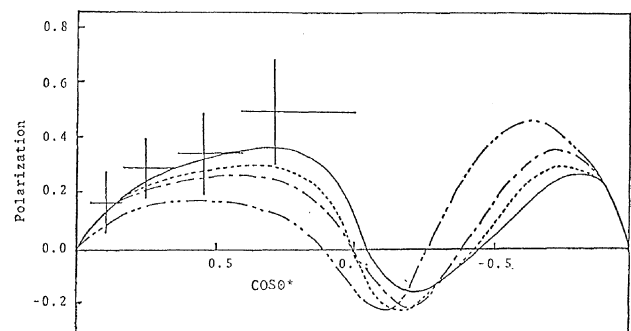


Fig. 22. Polarization in $\bar{p}p$ elastic scattering at 0.7 GeV/c. The curves represent predictions of the Bryan-Phillips model. Solid line: $g^2(\pi) = 15.0$, dotted line = 14.5, dot-dashed line = 14.0, dash-dot line = 12.66.

were selected out of 220 k pictures of 81-cm Saclay hydrogen BC exposed to the 0.7-GeV/c antiproton beams at CERN. From these events, the polarization parameters at four angles have been reduced and are shown in Fig. 22. The results are in good agreement with the theoretical predictions of the Bryan-Phillips model⁴² using OBEP with the π -N coupling-constant $g^2(\pi)=15.0$ instead of the original $g^2(\pi)=12.66$. This result is also supported with their DSC results of the pp charge-exchange scattering.

References

1. I. P. Auer *et al.*: paper 446, submitted to this Conference.
2. F. Halzen and G. H. Thomas: Phys. Rev. **D10** (1974) 344.
3. E. L. Berger, A. C. Irving and C. Sorensen: Phys. Rev. **D17** (1978) 2971.
4. E. Colton *et al.*: Nucl. Instr. and Methods **151** (1978) 85.
5. H. Becker *et al.*: paper 472, submitted to this Conference.
6. H. Kagen *et al.*: paper 461, submitted to this Conference.
7. Y. Makdisi *et al.*: paper 465, submitted to this Conference.
8. M. Sawamoto and S. Wakaizumi: Paper 775, submitted to this Conference.
9. J. R. O'Fallon *et al.*: Phys. Rev. Letters **39** (1977) 733.
10. H. DeKerrett *et al.*: Phys. Letters **62B** (1976) 363; **68B** (1977) 374.
11. D. G. Crabb *et al.*: paper 423, submitted to this Conference.
12. G. Baranko *et al.*: paper 680, submitted to this Conference.
13. M. E. Zeller *et al.*: paper 683, submitted to this Conference.
14. C. Bourrely, J. Soffer and T. T. Wu: Paper 80, submitted to this Conference.
15. G. Bunce *et al.*: Phys. Rev. Letters **36** (1976) 1113.
16. The sign of the polarization is determined by the authors according to the convention $\hat{n}=(\mathbf{P}_{\text{beam}} \times \mathbf{P}_X)/P_{\text{beam}} \times P_X$ which reduced to the Basel convention in the case of elastic scattering.
17. M. Concoran *et al.*: Phys. Rev. Letters **40** (1978) 1113.
18. K. Heller, Univ. of Michigan preprint (1977); G. L. Kane and Y. P. Yao: University of Michigan preprint UM HE 77-44 (1977).
19. I. P. Auer *et al.*: Phys. Rev. Letters **39** (1977) 313.
20. G. L. Kane and A. Siedl: Rev. mod. Phys. **48** (1976) 309.
21. C. W. Akerlof *et al.*: Phys. Rev. **D14** (1976) 2864; Fermilab Single Arm Spectrometer Group: Phys. Rev. Letters **35** (1975) 1195; N. Kwak *et al.*: Phys. Letters **58B** (1974) 233.
22. G. Fidecaro *et al.*: paper 715, submitted to this Conference.
23. J. Pumplin and G. Kane: Phys. Rev. **D11** (1976) 1183.
24. H. R. Gerhold and W. Majerotte: paper 692, submitted to this Conference.
25. A. Gaidot *et al.*: Phys. Letters **61B** (1976) 103.
26. J. Antille *et al.*: paper 663, submitted to this Conference.
27. C. Bourrely and J. Soffer: Phys. Letters **71B** (1977) 330.
28. C. K. Chen: to be published.
29. W. Beusch *et al.*: Phys. Letters **46B** (1973) 477.
30. A. de Lesquen *et al.*: paper 233, submitted to this Conference.
31. M. Borghini *et al.*: Phys. Letters **31B** (1970) 405; **36B** (1971) 497.
32. M. Fukushima *et al.*: paper 455, submitted to this Conference.
33. C. T. Coffin *et al.*: Phys. Rev. **159** (1967) 1169.
34. J. Banaigs *et al.*: Nucl. Phys. **B8** (1968) 31.
35. M. Fukushima *et al.*: paper 456, submitted to this Conference.
36. D. Hill *et al.*: Phys. Rev. Letters **26** (1971) 1241.
37. K. Miyake *et al.*: paper 544, submitted to this Conference.
38. R. Ayed *et al.*: Rev. of Particle Properties, Phys. Letters **50B** (1974).
39. R. M. Brown *et al.*: Nucl. Phys. **B117** (1976) 12; RL-76-093 Rutherford Lab. (1976).
40. G. Hohler *et al.*: TKP 78-10 (1978), TKP 78-11 (1978).
41. M. Kimura *et al.*: paper 569, submitted to this Conference.
42. R. J. N. Phillips: Rev. mod. Phys. **39** (1976) 681; R. A. Bryan *et al.*: Nucl. Phys. **B5** (1968) 201.